

Fake evolution of dark energy from observation data

Shi Qi*

Purple Mountain Observatory, Chinese Academy of Sciences, Nanjing 210008, China
Key Laboratory of Dark Matter and Space Astronomy,
Chinese Academy of Sciences, Nanjing 210008, China
Joint Center for Particle, Nuclear Physics and Cosmology,
Nanjing University—Purple Mountain Observatory, Nanjing 210093, China and
Kavli Institute for Theoretical Physics China, Chinese Academy of Sciences, Beijing 100190, China

The equation of state (EOS) of the dark energy is the key parameter to study the nature of the dark energy from the observation. Though the dark energy is found to be well consistent with the cosmological constant with a constant EOS of -1 , weak evidences from different observation data and analyses show that dark energy models with an evolving EOS slightly less than -1 at some medium redshifts and greater than -1 at high redshifts are more favored. In this paper, It is shown that how such a pattern of an evolving dark energy EOS can be just biases arising from the statistical method widely adopted in data analyses together with the dependence of the cosmic expansion on the dark energy EOS. The issue is actually not limited to dark energy or cosmology. It represents a class of mathematical problems of Bayesian analysis. It should be paid attention to in similar data analyses to avoid biases in drawing conclusions.

I. INTRODUCTION

Since the discovery the accelerating expansion of the universe [1, 2], which is attributed to the dark energy, the equation of state (EOS) of the dark energy have been, and will be for a long time in the future, the key parameter to study the nature of the dark energy from the observation. Though a constant dark energy EOS of -1 which corresponds to the cosmological constant is well consistent with the observation (see e.g. [3, 4] for recent analyses), weak evidences are persistently observed from different data sets that the dark energy EOS is slightly less than -1 at medium redshifts and greater than -1 at high redshifts. These evidences come from independent analyses of different kinds of data sets, including both standard candles like type Ia supernovae (SNe Ia) and gamma-ray bursts (GRBs) and standard rulers like baryon acoustic oscillations (BAO). See [5] for a comprehensive study showing this trend with SNe Ia, BAO, and other data sets and [6–8] for a series of studies showing that GRBs favor a dark energy EOS greater than -1 at high redshifts. See also [9, 10] for some recent studies with similar results. Interestingly, even mock data generated by assuming a Λ CDM cosmological model also show weak evidences for such a trend [11]. In this paper, It is shown that how the trend can be just biases resulted from the statistical method widely adopted in data analyses together with the dependence of the cosmic expansion on the dark energy EOS.

II. LUMINOSITY DISTANCE AND STANDARD CANDLES

We start from constructing the procedure for estimating constraints of standard candles on cosmological parameters using mock data. Consider a luminosity relation of the following form:

$$y = c_0 + \sum_i c_i x_i + \varepsilon, \quad (1)$$

where x_i s are some luminosity indicators which can be directly measured from observation, ε is a random variable accounting for the intrinsic scatter σ_{int} of the relation, and y has the form of

$$y = \log(4\pi d_L^2 \mathcal{F}), \quad (2)$$

where d_L is the luminosity distance and \mathcal{F} may be any physical quantity that can be directly measured from observation. The luminosity relation of Eq. (1) has incorporated all the GRB correlations summarized in [12], as well as the relations used to derived distance moduli from SNe Ia. For example, the SALT2 method [13] gives $\mu_B = m_B^* - M + \alpha \cdot x_1 - \beta \cdot c$. Let $y = (\mu_B - m_B^*)/2.5$, it can be rewritten in the form of Eq. (1). Note that the intrinsic scatter in distance modulus should be divided by 2.5 to convert to the intrinsic scatter σ_{int} in y .

From a similar derivation like that in [14], we know that, for a given sample of standard candles, the joint likelihood function for the coefficients c , the intrinsic scatter σ_{int} , and the cosmological parameters θ is

$$\mathcal{L}(c, \sigma_{\text{int}}, \theta) = k \prod_i \mathcal{L}_i, \quad (3)$$

where k is the normalization factor, i runs over the stan-

* qishi11@gmail.com

dard candles, and

$$\mathcal{L}_i = \frac{1}{\sqrt{\sigma_{\text{int}}^2 + \sigma_{y_i}^2 + \sum_j c_j^2 \sigma_{x_{j,i}}^2}} \times \exp \left[-\frac{\left(y_i - c_0 - \sum_j c_j x_{j,i} \right)^2}{2 \left(\sigma_{\text{int}}^2 + \sigma_{y_i}^2 + \sum_j c_j^2 \sigma_{x_{j,i}}^2 \right)} \right] \quad (4)$$

with j running over the luminosity indicators in Eq. (1). This likelihood function is a quite general one with the well known χ^2 statistic being a special case of it.

In the discussions below, we ignore the measurement uncertainties ($\sigma_{x_{j,i}}$ and σ_{y_i} in Eq. (4)) to simplify the problem.

First consider the simplest case. For the luminosity relation of

$$y = a + bx + \varepsilon, \quad (5)$$

to estimate its constraints on the cosmological parameters θ using mock data, we follow the following steps:

1. Set the fiducial values for the parameters of the luminosity relation a , b , σ_{int} and the cosmological parameters θ . Here, we use a_0 , b_0 , $\sigma_{\text{int},0}$, and θ_0 to denote the fiducial values for the corresponding parameters.
2. Generate the mock data for a sample of standard candles. Assume the total number of standard candles is N . For the i th standard candles, we generate its redshift z_i and luminosity indicator x_i and draw a sample ε_i from the distribution of random variable ε , i.e., the normal distribution $\mathcal{N}(0, \sigma_{\text{int},0}^2)$. From them we know its fiducial value for y :

$$y_{i,0} = a_0 + b_0 x_i + \varepsilon_i.$$

Then we calculate \mathcal{F}_i , i.e. the value of \mathcal{F} for individual standard candles that should be measured from the observation given the above information, through

$$y_{i,0} = \log [4\pi d_L^2(z_i, \theta_0) \mathcal{F}_i].$$

Thus, we can calculate y_i for any given cosmological parameters:

$$\begin{aligned} y_i &= \log [4\pi d_L^2(z_i, \theta) \mathcal{F}_i] \\ &= \log [4\pi d_L^2(z_i, \theta_0) \mathcal{F}_i] \\ &\quad - \log [d_L^2(z_i, \theta_0)] + \log [d_L^2(z_i, \theta)] \\ &= y_{i,0} + 2 \log [d_L(z_i, \theta) / d_L(z_i, \theta_0)] \\ &= a_0 + b_0 x_i + \varepsilon_i + 2 \log \frac{d_L(z_i, \theta)}{d_L(z_i, \theta_0)}. \end{aligned}$$

For later convenience, we define

$$l(z, \theta, \theta_0) = 2 \log \frac{d_L(z, \theta)}{d_L(z, \theta_0)} \quad (6)$$

and use l_i as the abbreviation for $l(z_i, \theta, \theta_0)$. So, we have

$$y_i = a_0 + b_0 x_i + \varepsilon_i + l_i.$$

3. Calculate the likelihood. Ignoring the measurement uncertainties, we have

$$\begin{aligned} \mathcal{L}_i &= \frac{1}{\sigma_{\text{int}}} \exp \left[-\frac{(y_i - a - bx_i)^2}{2\sigma_{\text{int}}^2} \right] \\ &= \frac{1}{\sigma_{\text{int}}} \exp \left[-\frac{(\delta a + \delta b x_i - \varepsilon_i - l_i)^2}{2\sigma_{\text{int}}^2} \right], \end{aligned}$$

where $\delta a \equiv a - a_0$ and $\delta b \equiv b - b_0$. Let $m_i = \delta b x_i - \varepsilon_i - l_i$, the joint likelihood function is

$$\begin{aligned} \mathcal{L}(a, b, \sigma_{\text{int}}, \theta) &= k \prod_{i=1}^N \mathcal{L}_i \\ &= \frac{k}{\sigma_{\text{int}}^N} \exp \left[-\frac{\sum_{i=1}^N (\delta a + m_i)^2}{2\sigma_{\text{int}}^2} \right] \\ &= \frac{k}{\sigma_{\text{int}}^N} \exp \left[-\frac{(\delta a)^2 + 2\overline{m}\delta a + \overline{m^2}}{2\sigma_{\text{int}}^2/N} \right], \end{aligned}$$

where \overline{m} and $\overline{m^2}$ are the average values of m and m^2 over the standard candles.

4. Marginalize out the nuisance parameters. Since we aim at constraining the cosmological parameters θ , we need integrate the joint likelihood function over the nuisance parameters. In this case, they are the calibration parameters a , b , and σ_{int} .

- (a) Integrate over the intercept parameter.

$$\begin{aligned} \mathcal{L}(b, \sigma_{\text{int}}, \theta) &= \int_{-\infty}^{+\infty} \mathcal{L}(a, b, \sigma_{\text{int}}, \theta) d\delta a \\ &= \frac{k}{\sigma_{\text{int}}^{N-1}} \sqrt{\frac{2\pi}{N}} \exp \left(-\frac{\sigma_m^2}{2\sigma_{\text{int}}^2/N} \right), \end{aligned}$$

where $\sigma_m^2 = \frac{1}{N} \sum_{i=1}^N (m_i - \overline{m})^2 = \overline{m^2} - \overline{m}^2$ is the variance of m .

- (b) Integrate over the slope parameter. Let $n_i = \varepsilon_i + l_i$, then $m_i = \delta b x_i - n_i$. Since x_i , ε_i , and l_i are independent of each other, we have

$$\sigma_m^2 = (\delta b)^2 \sigma_x^2 + \sigma_n^2.$$

Therefore

$$\begin{aligned} \mathcal{L}(\sigma_{\text{int}}, \theta) &= \int_{-\infty}^{+\infty} \mathcal{L}(b, \sigma_{\text{int}}, \theta) d\delta b \\ &= \frac{k}{\sigma_{\text{int}}^{N-2}} \frac{2\pi}{N} \frac{1}{\sigma_x} \exp \left(-\frac{\sigma_n^2}{2\sigma_{\text{int}}^2/N} \right). \end{aligned}$$

Note that σ_x here is the standard deviation of $\{x_i\}$, not the measurement uncertainty $\sigma_{x_{j,i}}$ in Eq.(4).

(c) Integrate over the intrinsic scatter.

$$\begin{aligned}\mathcal{L}(\theta) &= \int_0^{+\infty} \mathcal{L}(\sigma_{\text{int}}, \theta) d\sigma_{\text{int}} \\ &= \frac{k\pi}{N\sigma_x} 2^{\frac{N-3}{2}} \Gamma\left(\frac{N-3}{2}\right) (N\sigma_n^2)^{-\frac{N-3}{2}} \\ &\propto (\sigma_n^2)^{-\frac{N-3}{2}}.\end{aligned}$$

Here $\sigma_n^2 = \sigma_\varepsilon^2 + \sigma_l^2$, and σ_ε^2 is an estimation of $\sigma_{\text{int},0}^2$. So the marginal likelihood of the cosmological parameters θ is given by

$$\mathcal{L}(\theta) \propto (\sigma_{\text{int},0}^2 + \sigma_l^2)^{-\frac{N-3}{2}}.$$

For the general case of Eq. (1), the steps and the derivation are basically the same as the above. The step 4b can be repeated until all the slope parameters are integrated over. It is easy to check that the generalized marginal likelihood of the cosmological parameters θ is given by

$$\mathcal{L}(\theta) \propto (\sigma_{\text{int},0}^2 + \sigma_l^2)^{-\frac{N-p}{2}}, \quad (7)$$

where p is the number of the calibration parameters which include the coefficients c and the intrinsic scatter σ_{int} . This also applies to the case of no luminosity indicator, i.e., the case of the luminosity relation $y = a + \varepsilon$.

Thus, at this point, given a luminosity relation, we do not need to follow the above steps any more to estimate its constraints on cosmological parameters. Instead, we can directly calculate the marginal likelihood of the cosmological parameters using Eqs. (6) and (7) with the input of the number of luminosity indicators involved, the intrinsic scatter of the luminosity relation, and the number of the standard candles and their redshifts.

Throughout this paper to the end, if not stated explicitly otherwise, the flat Λ CDM with $\Omega_m = 0.3$ is used as the fiducial cosmological model. And since our focus is on the dark energy EOS $w(z)$, we fix all other cosmological parameters at their fiducial values. Thus $l(z, \theta, \theta_0)$ reduces to $l(z, w(z), -1)$. For the w CDM cosmological model where $w(z) = w$ is a constant along the redshift, it further reduces to $l(z, w, -1)$.

Now let us take a close look at $l(z, w, -1)$. From Eq. (6), it is easy to check that $l(z, w, -1)$ approaches 0 when z approaches 0 and, as long as $w < 0$, $l(z, w, -1)$ also approaches 0 when z approaches infinity. So $l(z, w, -1)$ has a maximum or minimum at some redshift where its differential with respect to z is equal to 0. See Fig. 1 (left panel) for examples of $l(z, w, -1)$ versus z for some values of w . For a given $w = w_{\text{np}}$, we can find the redshift, say z_{data} , where $dl(z, w, -1)/dz = 0$. Since σ_l^2 is the variance of $l(z, w, -1)$ along the redshift, if we only use standard candles distributing in a narrow redshift range around z_{data} , then σ_l , as a function of w , will show a local minimum at $w = w_{\text{np}}$ in addition to at the fiducial value $w = -1$. So, from Eq. (7), we know

that the marginal likelihood of w , $\mathcal{L}(w)$, will have local maxima at both $w = w_{\text{np}}$ and $w = -1$. See Fig. 2 for an illustration of two examples. The fiducial value $w = -1$ is what we want from the constraining, while $w = w_{\text{np}}$ is an irrelative non-physical value. A blind analysis without considering the impact of w_{np} could lead to biased conclusions in the constraining of the dark energy EOS. The relation between w_{np} and z_{data} for standard candles is plotted in Fig. 1 (right panel). We can see that w_{np} increases with the increase of z_{data} and crosses the fiducial value $w = -1$ at $z_{\text{data}} \simeq 1.3$. This means that, taking into account both the likelihood peaks corresponding to the fiducial value -1 and the non-physical value w_{np} , as was done implicitly in related analyses, the standard candles with redshifts less/greater than 1.3 would appear to favor a dark energy EOS less/greater than -1 . This is illustrated in Fig. 2.

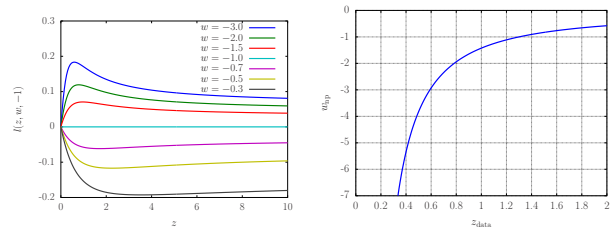


FIG. 1. $l(z, w, -1)$ versus z for some values of w and w_{np} versus z_{data} for standard candles.

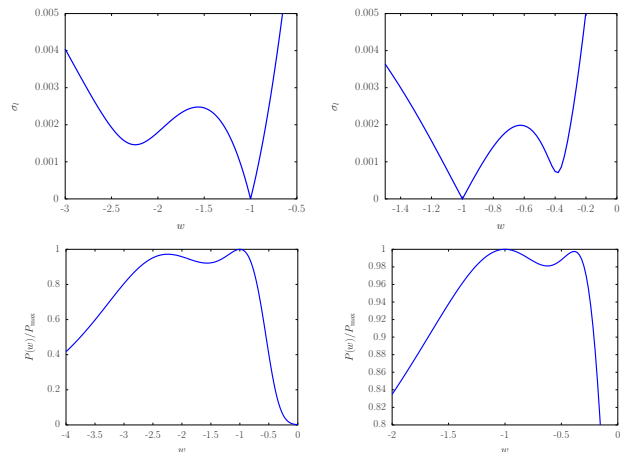


FIG. 2. σ_l versus w and the corresponding probability distribution of w . For the left column, 100 standard candles uniformly distributing in the redshift range $[0.5, 1]$ are used, and $\sigma_{\text{int},0} = 0.06$ and $p = 4$ are assumed for the luminosity relation. For the right column, 100 standard candles uniformly distributing in the redshift range $[2, 4]$ are used, and $\sigma_{\text{int},0} = 0.1$ and $p = 3$ are assumed for the luminosity relation.

With that the likelihood peak corresponding to w_{np} evolves with z_{data} while the one corresponding to the fiducial value does not, the impact of w_{np} actually would not be an issue if we use a sample of standard candles

with a wide redshift distribution and assume a constant dark energy EOS, since the likelihood peak corresponding to the fiducial value would be strengthened by standard candles at different redshifts while the one corresponding to w_{np} would be suppressed. However, when a flexible parameterization of the dark energy EOS allowing evolution along the redshift is used, which is a realistic demand to reconstruct the dark energy EOS from observation, the impact of w_{np} enters since, for these cases, the constraint of the dark energy EOS at a certain redshift mainly comes from only part of the standard candles at some redshifts. For z_{data} near to 0, w_{np} is far below the fiducial value $w = -1$, its impact in constraining usually has been implicitly eliminated by assuming that the dark energy EOS is not very far away from -1 . Thus, if the impact of w_{np} is significant enough, we can expect, from the constraining, a dark energy EOS that is around -1 at low redshifts, slightly biased to below -1 at medium redshifts, and slightly biased to greater than -1 at high redshifts. This is exactly the trend that is observed in different analyses [5–11]. The significance of the biased trend depends on, in addition to the redshift distribution of the data, the flexibility of the parameterization of the dark energy EOS. A less flexible parameterization means a stronger prior introduced, which may erase the bias if it is strong enough (an extreme example is the parameterization of a constant dark energy EOS along the redshift). However, a too flexible parameterization usually means large statistical errors, which could totally overwhelm the bias and make it not notable. Especially for cases with a poorly constrained dark energy EOS at high redshifts, the likelihood there usually has a long wing at the lower end (since the data does not care much about the value of the dark energy EOS at high redshifts as long as the matter dominance is guaranteed, which means only an upper limit is imposed on the dark energy EOS), which could make the dark energy EOS at high redshifts appear less than -1 instead of greater than -1 . The relation between the significance of the trend and the parameterization of the dark energy EOS is very subtle. A principal component analysis [15] of $1 + w(z)$ utilizing Eqs. (6) and (7) is presented in Fig. 3. It shows that the best constrained components do reflect the impact of w_{np} with w biased toward less than -1 at medium redshifts, which is consistent with the result of similar analyses derived from real data [10]. (The best constrained components do not include the variation of the dark energy EOS at high redshifts, so the bias from w_{np} at high redshifts does not show up here.) It can be expected that, if the prior introduced by some parameterization of the dark energy EOS and/or extra data effectively suppress the poorly constrained components while retaining the best constrained components, the bias from w_{np} will be visible in the final result. For example, Fig. 2 (Panels A1, A2) in [5] shows that only the 2(3) strongest data modes survive the addition of the prior there, thus, when compared with the result here derived from the fiducial model of the cosmological constant, the favor of the dynamical

dark energy in [5] is understandable as a result of the impact of w_{np} .

It should be also noted that, when using Eqs. (6) and (7), the problem has been simplified in a few places. For example, the measurement uncertainties are ignored and the covariance between x , ε , and l are assumed to be exactly zero (Though it is expected to be true, real data are usually not so ideal). How these simplifications impact on the constraining of the evolution of the dark energy EOS need further investigation. For a precise comparison with results derived from real data, they may have an unignorable effect and should be taken into account. And in practice, standard candles are usually handled differently in different analyses before used to constrain cosmological parameters, which is another thing need to be considered.

III. GENERALIZATION

It is easy to see that the above discussions can be applied to more than just luminosity distance and standard candles. In fact, Eq. (2) can be generalized to

$$y = \log [X(z, \theta)\mathcal{F}], \quad (8)$$

where $X(z, \theta)$ can be anything to be measured from the observation that depends on cosmological parameters. All the subsequent derivations are of the same, except that the definition of $l(z, \theta, \theta_0)$, Eq. (6), is generalized to

$$l(z, \theta, \theta_0) = \log \frac{X(z, \theta)}{X(z, \theta_0)}. \quad (9)$$

The form of Eq. (7) remains unchanged. Thus, the results are generalized to other observations.

For BAO survey, the comoving sound horizon at the baryon drag epoch, $r_s(z_{\text{drag}})$, is used as the standard ruler. For the standard ruler of the transverse direction, of the line-of-sight direction, and of the combined directions, the following distance ratios are measured from the survey respectively:

$$\theta_s = \frac{r_s(z_{\text{drag}})}{(1+z)d_A}, \quad (10)$$

$$\delta z_s = \frac{r_s(z_{\text{drag}})H(z)}{c}, \quad (11)$$

$$d_s = \frac{r_s(z_{\text{drag}})}{D_V}. \quad (12)$$

These relations can be rewritten in the form of $y = a + \varepsilon$ with $a = \log[r_s(z_{\text{drag}})]$, \mathcal{F} being θ_s , δz_s , and d_s respectively, and $X(z, \theta)$ being $(1+z)d_A$, $c/H(z)$, and D_V respectively. Thus, $l(z, \theta, \theta_0)$ can be calculated from Eq. (9) and corresponding w_{np} can be derived from it. (Here, only BAO measurements from density fluctuations of baryonic matter are considered, no prior information about $r_s(z_{\text{drag}})$ from cosmic microwave background (CMB) measurements is inputted. $r_s(z_{\text{drag}})$ is

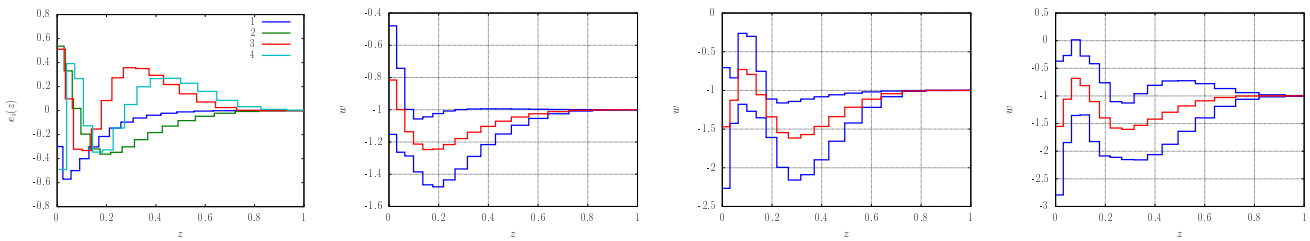


FIG. 3. Principal component analysis [15] of $1 + w(z)$. $w(z)$ was parameterized using 20 bins with a constant bin width of 0.03 in scale factor within $[0.4, 1]$ and $|1 + w(z)| \leq 50$ was assumed. Mock SN Ia data ($\sigma_{\text{int},0} = 0.06$ and $p = 4$) together with mock GRB data ($\sigma_{\text{int},0} = 0.4$ and $p = 3$) were used. The mock SN Ia data has the same redshifts of SNLS3 data [16] and the mock GRB data has the same redshifts of the sample in [8]. From left to right, the 4 best constrained components of $1 + w(z)$ are plotted in the first panel (Small shifts in z are applied to the components to reduce the overlap of the lines so that the components are presented more clearly). In the following panels, the median values (red lines) and the 1σ confidence intervals (blue lines) of $w(z)$ reconstructed from the 2, 3, and 4 best constrained components of $1 + w(z)$ are plotted.

treated as an unknown constant and simply marginalized during the constraining. For example, in [17, 18], part of the BAO measurements are summarized in distance ratio $D_V(0.35)/D_V(0.2)$, which is effectively equivalent to marginalizing out $r_s(z_{\text{drag}})$ if used to constrain the dark energy EOS. If BAO measurements are combined with CMB measurements, such that the information about $r_s(z_{\text{drag}})$ is inputted, the impact of w_{np} should be relieved or eliminated.) Since the luminosity distance d_L and the angular diameter distance d_A relate to each other though $d_L = d_A(1+z)^2$, the $l(z, \theta, \theta_0)$ for the standard ruler of the transverse direction differs from that for standard candles only by a constant factor of 2. So the derived w_{np} is totally the same. For the other two cases, i.e., the standard ruler of the line-of-sight direction and of the combined directions, w_{np} versus z_{data} is plotted in Fig. 4. We can see similar behaviors of w_{np} versus z_{data} . w_{np} crosses the fiducial dark energy EOS at different values of z_{data} . For the former case, at $z_{\text{data}} \simeq 0.65$, and for the latter one, at $z_{\text{data}} \simeq 0.9$.

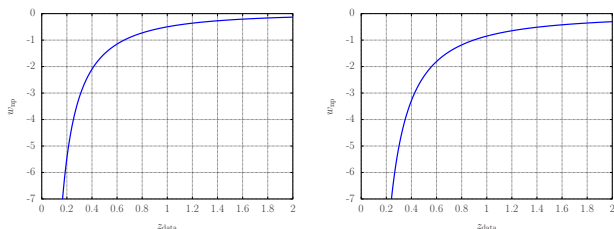


FIG. 4. w_{np} versus z_{data} for the standard ruler of the line-of-sight direction (left) and of the combined directions (right).

To be more general, what were discussed here is not limited to dark energy or cosmology. In fact, it represents a class of mathematical problems of Bayesian analysis. Fitting data to a linear relation and using the relation to constrain model parameters are very common in data analyses. The key quantity in the discussions, σ_l , appears during the marginalization (it shows up in 4a through σ_m when we integrate over the intercept parameter), which

is almost inevitable in data analyses. So similar biases may show their shadow here and there in similar problems. Concerning data analyses in cosmology, a lot of parameters are involved. Marginalization is used very often. The kind of bias discussed here should be checked carefully in the era of precision cosmology.

IV. SUMMARY

Starting with luminosity relations of standard candles, the steps was described that one should follow to estimate the constraints of a luminosity relation on cosmological parameters using mock data, from which a simple and general formula was deduced that can be used to directly calculate the marginal likelihood of cosmological parameters. Using the formula together with the dependence of the cosmic expansion on the dark energy EOS, it was shown how a kind of bias could arise that leads to a fake evolution of the dark energy EOS, whose significance depends on the flexibility of the parameterization of the dark energy EOS and the redshift distribution of the data. Then the formula was generalized to more than just standard candles. It was shown that the BAO data could lead to similar biases. It was mentioned that the issue represents a class of mathematical problems of Bayesian analysis and should be paid attention to in similar analyses.

ACKNOWLEDGMENTS

This work was supported by the National Natural Science Foundation of China (Grant No. 10973039, 11203079, and 11373068), Key Laboratory of Dark Matter and Space Astronomy (Grant No. DMS2011KT001), and the Project of Knowledge Innovation Program (PKIP) of Chinese Academy of Sciences (Grant No. KJCX2.YW.W10).

-
- [1] A. G. Riess *et al.* (Supernova Search Team), *Astron. J.* **116**, 1009 (1998), astro-ph/9805201.
- [2] S. Perlmutter *et al.* (Supernova Cosmology Project), *Astrophys. J.* **517**, 565 (1999), astro-ph/9812133.
- [3] P. Ade *et al.* (Planck), (2015), arXiv:1502.01589 [astro-ph.CO].
- [4] P. Ade *et al.* (Planck), (2015), arXiv:1502.01590 [astro-ph.CO].
- [5] G.-B. Zhao, R. G. Crittenden, L. Pogosian, and X. Zhang, *Phys.Rev.Lett.* **109**, 171301 (2012), arXiv:1207.3804 [astro-ph.CO].
- [6] S. Qi, F.-Y. Wang, and T. Lu, *Astron. Astrophys.* **483**, 49 (2008), arXiv:0803.4304 [astro-ph].
- [7] S. Qi, T. Lu, and F.-Y. Wang, *Mon. Not. Roy. Astron. Soc.* **398**, L78 (2009), arXiv:0904.2832 [astro-ph.CO].
- [8] F. Wang, S. Qi, and Z. Dai, *Mon. Not. Roy. Astron. Soc.* **415**, 3423 (2011), arXiv:1105.0046 [astro-ph.HE].
- [9] Y. Hu, M. Li, X.-D. Li, and Z. Zhang, *Sci.China Phys.Mech.Astron.* **57**, 1607 (2014), arXiv:1401.5615 [astro-ph.CO].
- [10] W. Zheng, S.-Y. Li, H. Li, J.-Q. Xia, M. Li, *et al.*, *JCAP* **1408**, 030 (2014), arXiv:1405.2724 [astro-ph.CO].
- [11] D. Sarkar, S. Sullivan, S. Joudaki, A. Amblard, D. E. Holz, and A. Cooray, *Phys. Rev. Lett.* **100**, 241302 (2008), arXiv:0709.1150 [astro-ph].
- [12] S. Qi and T. Lu, *Astrophys.J.* **749**, 99 (2012), arXiv:1111.6249 [astro-ph.CO].
- [13] J. Guy, P. Astier, S. Baumont, D. Hardin, R. Pain, *et al.*, *Astron.Astrophys.* **466**, 11 (2007), arXiv:astro-ph/0701828 [ASTRO-PH].
- [14] G. D'Agostini, (2005), arXiv:physics/0511182.
- [15] D. Huterer and G. Starkman, *Phys. Rev. Lett.* **90**, 031301 (2003), astro-ph/0207517.
- [16] A. Conley *et al.* (SNLS), *Astrophys.J.Suppl.* **192**, 1 (2011), arXiv:1104.1443 [astro-ph.CO].
- [17] W. J. Percival *et al.*, *Mon. Not. Roy. Astron. Soc.* **381**, 1053 (2007), arXiv:0705.3323 [astro-ph].
- [18] W. J. Percival *et al.* (SDSS), *Mon. Not. Roy. Astron. Soc.* **401**, 2148 (2010), arXiv:0907.1660 [astro-ph.CO].